Stability of a Servomechanism Operated by PWM Mode

By

Taizo Sawamura* and Hideo Hanafusa**

(Received July 31, 1962)

In a servomechanism operated by the PWM mode, the output contains the dither corresponding to the carrier pulse. When the loop gain becomes high, the dither component is fed back and modulates the pulse width. Therefore, we must consider not only the ordinary stability problem of the servo loop but also the stability of the dither.

First, the stability of the fundamental circuit was analyzed. In this case, it was shown that the various waveshapes took place depending on the ratio of the pulse transmission lag to the pulse period and the loop gain. The ranges of the loop gain were also obtained for various waves.

Next, the stability was studied with regard to the servomechanism in which two types of compensating circuits were used. One was a first-order system and the other was a phase lead network. It was shown that these compensating circuits were effective for stabilizing the servomechanism, if they were selected properly. The optimum time constants were obtained for these compensating circuits.

Finally, the theoretical results were verified by experiments which were carried out by an electrohydraulic servomechanism.

1. Introduction

Servomechanism are classified into two types: a continuous operation type and a relay control type. In the continuous operation type, the complexity and the high accuracy of the apparatus are required for reliable operation. In the relay control type, the construction is much simpler than the former, but accurate control is not expected on account of the hunting which is inevitable in a high gain loop.

In the servomechanism operated by the PWM mode, a pulse-width-modulation unit is added to the relay control system and the characteristics become similar to those of the servomechanism which operates as a continuous type for small inputs and operates as a relay control system for large inputs. Therefore, a high accuracy control is realized by comparatively simple construction[1],[2].

* Automation Research Laboratory
** Faculty of Industrial Arts, Kyoto Technical University

As the controlled system is driven by pulsative inputs in the PWM operation, the controlled output consists of two components. One is the output corresponding to the command to the servo loop, the other being the dither which has the same period as the carrier pulse. When the loop gain becomes high, the dither component which is fed back through the feedback circuit modulates the pulse width, and the dither in the output becomes unstable. Therefore, we should consider not only the ordinary stability problem of the servo loop but also the stability of the dither in the output.

In this paper, the stability problems of the servomechanism operated by the PWM mode are discussed for the fundamental circuit in which the feedback circuit consists of a proportional element. Next, a first-order system and two types of phase lead networks are used in a feedback circuit and the effects of these compensating circuits are compared. The validity of the analysis is verified by experiments which are carried out by an electrohydraulic servomechanism.

2. Construction and operation of a servomechanism operated by PWM mode

Fig. 1 shows a schematic diagram of the servomechanism operated by the PWM mode. The PWM unit generates the pulses as shown in Fig. 2 (a) for no
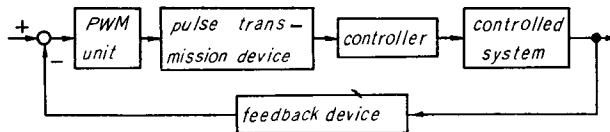
Fig. 1. Construction of a servomechanism operated by a PWM mode.

error signals. When the error signals are given, it is assumed that the modulated pulse train has the same period as the pulse train for no error signals, and that the widths of the positive pulses are modulated symmetrically on both sides of their centers in proportion to the momentary values of the error at the centers of the positive pulses. Fig. 2 (b) shows the pulses for error signals. Such modulation is said to be a symmetrical modulation of the pulse width, and it is a basic mode of the pulse-width-modulation for theoretical treatment. Such a mode of the modulation can not be realized by physical means in the strict sense of
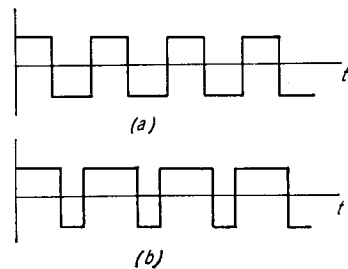
Fig. 2. Pulse generated in a PWM unit.

the term, but is realized approximately by the
following principle. Fig. 3 shows the error
signal and the pulse train in (a) and (b), re-
spectively. In this figure, T_1, $\overline{T}_1$ and T_2 show
the time lengths. E_1, $\overline{E}_1$ and E_2 are the aver-
age values of the error signal during each
durations. If the period of the unmodulated
pulse is T_0, the following relations exists :

Fig. 3.   Error signal and pulse train.

$$T_1 = (T_0/2)(1+kE_1) \tag{1}$$
$$\overline{T}_1 = (T_0/2)(1-k\overline{E}_1) \tag{2}$$
$$T_2 = (T_0/2)(1+kE_2) . \tag{3}$$

where k is the gain of modulation. In Fig. 3, A and B represent the centers of
pulses. The time length between A and B is obtained as

$$\frac{T_1}{2}+\frac{T_2}{2}+\overline{T}_1 = T_0+\frac{T_0}{4}k(E_1+E_2-2\overline{E}_1) . \tag{4}$$

If the error signal is represented by a rectilinear line, E_1 and E_2 represent
the error values at the moments corressponding to A and B, and the pulse period
does not change by Eq. (4). Therefore, symmetrical modulation can be realized
in this case. However, it can be realized approximately when the error signals
change otherwise than the rectilinear line.

The pulse excited by the PWM unit is transmitted to the controller through
the pulse transmission device, and the pulsative inputs are given to the controlled
system.

3.   Stability of a dither when a feedback circuit consists of a proportional element

Fig. 4 shows a block diagram
of the basic circuit of the servo-
mechanism in which the feedback
circuit consists of a proportional
element. In Fig. 4, t_{D0} represents
the pulse transmission lag, K_v and
K_f being the gain constants of the
controller and the feedback circuit, respectively.
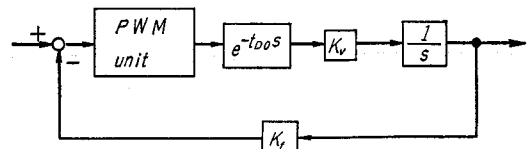

Fig. 4.   Block diagram of a fundamental circuit
operated by a PWM mode.

3.1.   Wave-shape change of a dither for $t_{D0} < T_0/2$

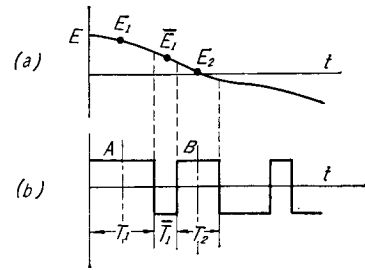In practical use, the most important is the case when the pulse transmission

lag t_{D_0} is smaller than a half period of the carrier pulse, $T_0/2$. In this case, the following waves exist as the dither in the output according to the loop gain.

(1)   Disturbed wave of a period $2T_0$

Fig. 5 shows the disturbed wave of a period $2T_0$. In Fig. 5, I and II are points on the output at the sampling instants, and are called "sampling points" from now on. The pulse widths excited by the PWM unit are modulated proportionally to the displacements of the sampling points, transmitted to the controller accompanying the lag t_{D_0},
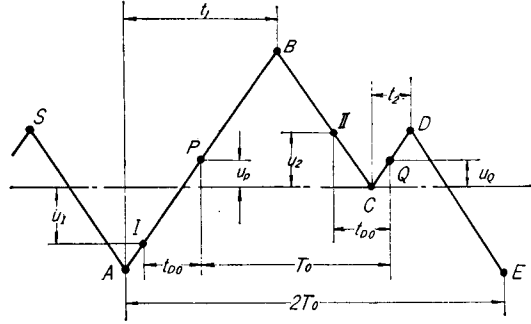

Fig. 5.   Disturbed wave of a period $2T_0$.

and then integrated by the integral properties of the controlled system. The integrated pulses are represented by **AB** and **CD** of Fig. 5. **P** and **Q** are the centers of **AB** and **CD**, respectively. If the notations are used as shown in Fig. 5, the following relations are obtained:

$$t_1 = (T_0/2)(1+K_f k u_1) \tag{5}$$

$$t_2 = (T_0/2)(1+K_f k u_2) \tag{6}$$

$$t_1+t_2 = T_0. \tag{7}$$

From Eqs. (5), (6) and (7),

$$u_2 = -u_1. \tag{8}$$

If v_m is used to denote the velocity, the positive direction of which is taken downward in the figure,

$$u_Q = u_P + v_m\{T_0-(t_1+t_2)\} = u_P. \tag{9}$$

When a disturbed wave takes place, it is proved easily that only the wave of Fig. 5 is the stationary wave, where the first sampling point exists on **AP** and the second sampling point exists on **BC**. From Fig. 5, the following relations are obtained:

$$u_1 = u_P + v_m t_{D_0} \tag{10}$$

$$u_2 = u_Q - v_m(t_{D_0}-t_2). \tag{11}$$

From Eqs. (7)~(11),

$$u_1 = -u_2 = \frac{v_m(4t_{D_0}-T_0)}{4-T_0 v_m K_f k}. \tag{12}$$

Now, u_1 must satisfy the following relations:

$$1 > K_f k u_1 > 0 \tag{13}$$

$$t_{D_0} > t_2/2 \tag{14}$$

$$t_{D_0} < t_1/2 . \tag{15}$$

Substituting Eq. (12) into Eqs. (13), (14) and (15), the conditions where the disturbed stationary wave of Fig. 5 exists are obtained as follows:

when $\quad T_0/2 > t_{D_0} > T_0/4$,

$$T_0/t_{D_0} > T_0 v_m K_f k > 2 .$$

when $\quad t_{D_0} < T_0/4$,

$$T_0 v_m K_f k > T_0/t_{D_0} . \tag{16}$$

Next, the stability of the disturbed wave of Fig. 5 will be studied. The solid lines in Fig. 6 show the same wave as in Fig. 5, and the broken lines show the wave which will occur by a small disturbance added to the stationary wave. From Fig. 6, the following relations are obtained:
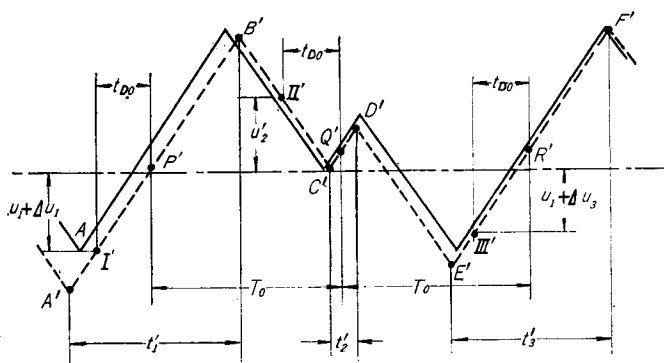

Fig. 6. Stability of a disturbed wave of a period $2T_0$.

$$t_1' = (T_0/2)\{1 + K_f k(u_1 + \Delta u_1)\} \tag{17}$$

$$t_2' = (T_0/2)(1 + K_f k u_2') \tag{18}$$

$$t_3' = (T_0/2)\{1 + K_f k(u_1 + \Delta u_3)\} \tag{19}$$

$$u_2' = (u_1 + \Delta u_1) - v_m\left(t_{D_0} + \frac{t_1'}{2}\right) + v_m\left\{T_0 - \left(t_{D_0} + \frac{t_1'}{2}\right)\right\} \tag{20}$$

$$u_1 + \Delta u_3 = u_2' - v_m\left(t_2' + \frac{t_3'}{2} - t_{D_0}\right) + v_m\left\{T_0 - \left(t_2' + \frac{t_3'}{2} - t_{D_0}\right)\right\} , \tag{21}$$

where Δu_1 and Δu_3 are the differences of displacements between the solid lines and the broken lines at the first and the third sampling points, respectively. From Eqs. (17)∼(21), the following relation is obtained:

$$\Delta u_3(2 + T_0 v_m K_f k) = \Delta u_1(2 - T_0 v_m K_f k)(1 - T_0 v_m K_f k) \tag{22}$$

$|\Delta u_3|$ must be smaller than $|\Delta u_1|$, in order that the solid wave is stable. Using

Eq. (22), the condition for $|\varDelta u_3| < |\varDelta u_1|$ leads to

$$0 < T_0 v_m K_f k < 4 .\tag{23}$$

From Eqs. (16) and (23), it is concluded that the stationary disturbed wave for $T_0/2 > t_{D0} > T_0/4$ is stable and the wave for $t_{D0} < T_0/4$ is unstable. The stable wave exists practically, but the unstable one does not occur.

(2) Triangular wave of a period T_0

The stable triangular waves are shown by the solid lines of Fig. 7 and Fig. 8 for the cases of $t_{D0} < T_0/4$ and $T_0/4 < t_{D0} < T_0/2$, respectively. In these cases, as the displacements at the sampling points should be zero, then

$$u_1 = u_2 = 0 .\tag{24}$$

Fig. 7. Triangular wave of a period T_0 for $t_{D_0} < T_0/4$.
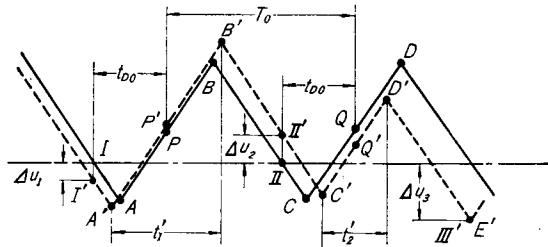
Fig. 8. Triangular wave of a period T_0 for $T_0/4 < t_{D_0} < T_0/2$.

Stabilities of these waves are studied as follows. The broken lines of Fig. 7 and Fig. 8 show the waves which will occur by small disturbances added to the stationary waves. The relations between $\varDelta u_1$ and $\varDelta u_2$ become as follows in each case:

For $t_{D0} < T_0/4$,

$$\varDelta u_2 = \frac{2 - T_0 v_m K_f k}{2 + T_0 v_m K_f k} \varDelta u_1 .\tag{25}$$

For $T_0/4 < t_{D0} < T_0/2$,

$$\varDelta u_2 = \varDelta u_1 (1 - T_0 v_m K_f k) .\tag{26}$$

From Eq. (25), $|\varDelta u_2|$ is always smaller than $|\varDelta u_1|$, and the stationary triangular wave of the period T_0 is always stable for $t_{D0} < T_0/4$. From Eq. (26), however, $|\varDelta u_2|$ is smaller than $|\varDelta u_1|$ only for $T_0 v_m K_f k < 2$, and it is concluded for $T_0/4 < t_{D0} < T_0/2$ that the stationary wave is stable for $T_0 v_m K_f k < 2$ and is unstable for $T_0 v_m K_f k \geqq 2$.

(3) Triangular wave of a period $2T_0$

The stable triangular wave is shown by the solid lines in Fig. 9 for $t_{D0} < T_0/2$. In this case, the following relations hold:
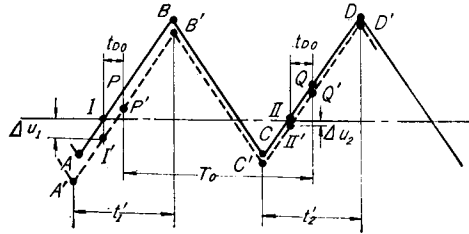
$$K_f k u_1 \geqq 1 \qquad (27)$$

$$K_f k u_2 \leqq -1 \qquad (28)$$

$$u_1 - u_P = u_P - u_2 = v_m t_{D0}. \qquad (29)$$

From Eqs. (27) and (29),

$$K_f k (v_m t_{D0} + u_P) \geqq 1. \qquad (30)$$

From Eqs. (28) and (29),

$$K_f k (v_m t_{D0} - u_P) \geqq 1. \qquad (31)$$

At the limit where the triangular wave of the period $2T_0$ takes place, the notation "$=$" is used in Eqs. (30) and (31), and they lead to $u_P = 0$ and $t_{D0} v_m K_f k = 1$. There-

Fig. 9. Triangular wave of a period $2T_0$.

fore, the condition where the stationary triangular wave of the period $2T_0$ exists is given by

$$T_0 v_m K_f k \geqq T_0 / t_{D0}. \qquad (32)$$

Next, the stability of the triangular wave will be studied. In this case, it should be considered separately for $\Delta u_1 > 0$ and for $\Delta u_1 < 0$, where Δu_1 is the disturbance given at the first sampling point. If Eqs. (27) and (28) still hold for Δu_1, it is obvious that the triangular wave of a period $2T_0$ is maintained and the stationary wave is stable. If Eq. (28) does not hold for positive Δu_1, the transient wave is shown by the broken lines of Fig. 9. In this figure, the following relation is obtained :

$$u_E'' = u_A' - T_0 v_m (1 + K_f k u_2') \qquad (33)$$

where u_E'', u_A' and u_2' are the displacements at points E'', A' and II' of Fig. 9, respectively. Substituting $u_A' = u_A + \Delta u_1$ in Eq. (33) leads to

$$u_E'' = u_A + \Delta u_1 (1 - T_0 v_m K_f k) - T_0 v_m (K_f k u_2 + 1) \qquad (34)$$

where u_A is the displacement of a point A of Fig. 9. Using $K_f k u_2 \leqq -1$, it is concululded that $u_A < u_E'' < u_A'$ for small Δu_1, and that the transient wave approaches the stationary wave gradually.

If Eq. (27) does not hold for negative Δu_1, the transient wave becomes the same as shown by the broken lines of Fig. 6. In this case, it is proved by the same method as for $\Delta u_1 > 0$ that the transient wave approaches the stationary wave gradually.

The results of the above analysis are shown in Table 1. When two stable waves exist for the same gain, either wave occurs according to the initial conditions.
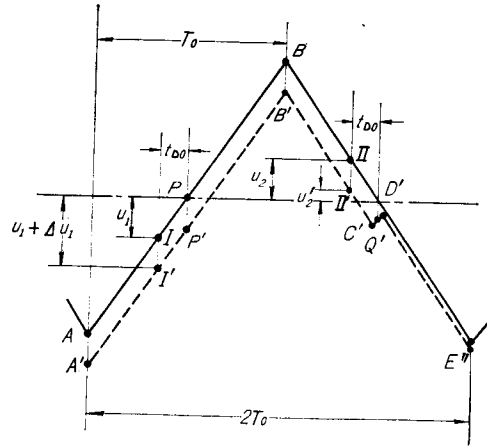
Table 1. Critical conditions for a waveshape-change.

t_{D_0}/T_0	$T_0 v_m K_f k$	Waveshape		Period
$t_{D_0}/T_0 < 1/4$	$T_0 v_m K_f k < T_0/t_{D_0}$	triangular	stable	T_0
	$T_0 v_m K_f k \geqq T_0/t_{D_0}$	triangular	stable	T_0
		disturbed	unstable	$2T_0$
		triangular	stable	$2T_0$
$1/4 < t_{D_0}/T_0 < 1/2$	$T_0 v_m K_f k < 2$	triangular	stable	T_0
	$2 \leqq T_0 v_m K_f k < T_0/t_{D_0}$	triangular	unstable	T_0
		disturbed	stable	$2T_0$
	$T_0 v_m K_f k \geqq T_0/t_{D_0}$	triangular	unstable	T_0
		triangular	stable	$2T_0$

3. 2. Some consideration for $t_{D_0} > T_0/2$

Though the most important case is $t_{D_0} < T_0/2$, t_{D_0} may become larger than $T_0/2$ when the pulse transmission device has a multi-stage amplifier. Also, the analysis for $t_{D_0} > T_0/2$ is useful in analyzing the characteristics of the servomechanism when the feedback circuit does not consist of a proportional element. In both cases, the practically important problem is to obtain the range of the loop gain in which only the triangular wave of the period T_0 can exist.

(1) The case of $3T_0/4 > t_{D_0} > T_0/2$

In this case, the triangular wave of the period T_0 is shown in Fig. 10. This figure is similar to that for $T_0/2 > t_{D_0} > T_0/4$, and the triangular wave of the period T_0 is stable for $T_0 v_m K_f k < 2$ and is unstable for $T_0 v_m K_f k \geqq 2$. When the triangular wave becomes unstable, the disturbed wave shown in Fig. 11 takes place and it is
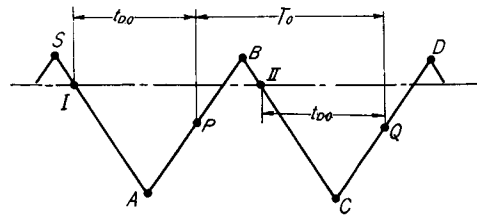

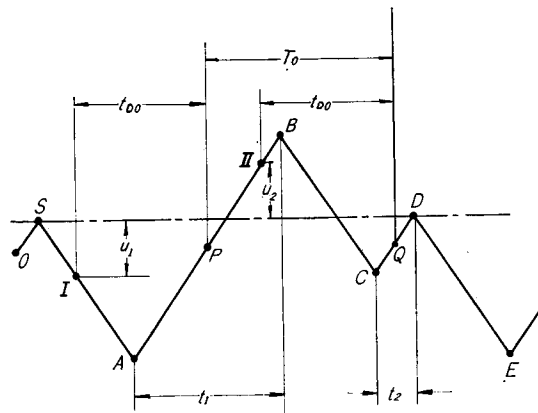Fig. 10. Triangular wave of a period T_0 for $T_0/2 < t_{D_0} < 3T_0/4$.

Fig. 11. Disturbed wave of a period $2T_0$ for $T_0/2 < t_{D_0} < 3T_0/4$.

stable for $2 \leq T_0 v_m K_f k < T_0 / (T_0 - t_{D0})$.

(2) The case of $T_0 > t_{D0}$
$> 3T_0/4$

In this case, the triangular wave of the period T_0 is shown by solid lines in Fig. 12. The broken lines in the same figure show the wave which will occur by small disturbances. From Fig. 12, the following relation is obtained:
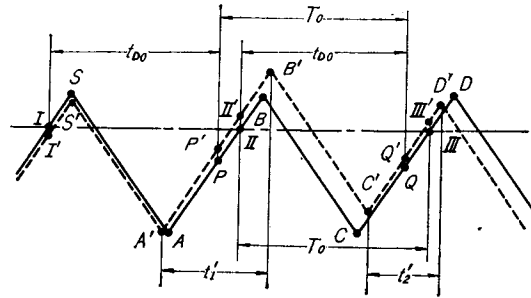

Fig. 12.   Trianguar wave of a period T_0 for $3T_0/4 < t_{D0} < T_0$.

$$\varDelta u_3 = \varDelta u_2 - \frac{1}{2} T_0 v_m K_f k (\varDelta u_1 + \varDelta u_2) . \tag{35}$$

As $|\varDelta u_3|$ is not always smaller than $|\varDelta u_1|$ even for small values of $T_0 v_m K_f k$, the triangular wave of the period T_0 is not stable for $t_{D0} > 3T_0/4$.

4. Stability of a servo loop and a dither when compensating circuits are used in a feedback circuit

Fig. 13 shows a block diagram of a fundamental circuit operated by the PWM mode, where $G_f(s)$ represents the transfer function of a compensating circuit. With respect to the stability of this servome-chanism, two problems must be considered:

Fig. 13.   Block diagram of a compensated circuit.

one is the stability of the servo loop, the other being the stability of the dither in the output.

4. 1. Stability of a servo loop

The stability limit of the servo loop is obtained by using the equivalent transfer function for the PWM unit. The equivalent frequency transfer function $G_d(j\omega)$ for the error signal of $E_a \sin \omega t$ is represented as follows[3]:

$$G_d(j\omega) = \frac{y_m}{E_a} \frac{8}{\omega T_0} \cos \left(\frac{\omega T_0}{4} \right) J_1 \left(\frac{k E_a \omega T_0}{4} \right), \tag{36}$$

where y_m is a height of the pulse. ωT_0 must be smaller than π in Eq. (36), because the PWM operation is a sort of sampling operation and the transfer function can be defined only for $\omega T_0 < \pi$. For the calculation of the stability limit, the input amplitude is considered to be small, and therefore Eq. (36) reduces to

$$G_d(j\omega) = k y_m \cos\left(\frac{\omega T_0}{4}\right). \tag{37}$$

Using the equivalent transfer function, the characteristic equation of the servo loop becomes as follows at the limit of stability:

$$1 + G_d(j\omega_l) \frac{K_v}{j\omega_l} G_f(j\omega_l) e^{-j\omega_l t_{D0}} = 0 \tag{38}$$

where ω_l is the angular frequency of the self-excited oscillation at the stability limit. It is seen from Eq. (37) that $G_d(j\omega_l)$ represents the gain depending upon ω_l and does not contain any phase shifts. Then, Eq. (38) is equivalent to the following two equations:

$$\omega_l t_{D0} - \angle G_f(j\omega_l) = \pi/2 \tag{39}$$

$$K_v G_d(j\omega_l) |G_f(j\omega_l)| = \omega_l. \tag{40}$$

As $G_d(j\omega_l)$ is defined only for $\omega_l T_0 < \pi$, Eqs. (39) and (40) are significant only for the same range of ω_l.

4.2. Stability of a dither in the output

The stability of the dither in the output for the case when the feedback circuit does not consist of a proportional element may be discussed approximately by extending the result of calculations for the case when the feedback circuit consists of a proportional element. The stability limits of the dither for the feedback circuit of the proportional element are given as follows:

When $t_{D0}/T_0 < 1/4$,

$$T_0 v_m K_f k = T_0/t_{D0}. \tag{41}$$

When $1/4 < t_{D0}/T_0 < 3/4$,

$$T_0 v_m K_f k = 2. \tag{42}$$

For the case when the compensating circuit is used in the feedback circuit, the stability limits are obtained approximately by substituting $G_f(j2\pi/T_0)$ for K_f and $\{t_{D0} - (T_0/2\pi)\angle G_f(j2\pi/T_0)\}$ for t_{D0} in Eqs. (41) and (42). The stability limits are given as follows by these approximations:

When $\left\{t_{D0} - \frac{T_0}{2\pi} \angle G_f\left(j\frac{2\pi}{T_0}\right)\right\} < \frac{T_0}{4}$,

$$\left\{t_{D0} - \frac{T_0}{2\pi} \angle G_f\left(j\frac{2\pi}{T_0}\right)\right\} v_m k \left|G_f\left(j\frac{2\pi}{T_0}\right)\right| = 1. \tag{43}$$

When $\frac{T_0}{4} < \left\{t_{D0} - \frac{T_0}{2\pi} \angle G_f\left(j\frac{2\pi}{T_0}\right)\right\} < \frac{T_0}{2}$,

$$T_0 v_m k \left|G_f\left(j\frac{2\pi}{T_0}\right)\right| = 2. \tag{44}$$

In designing the servomechanism, both the servo loop and the dither must

be stable. Therefore, the gain of the servo loop should be smaller than the critical gains calculated by Eqs. (40), (43) and (44).

5. Compensating circuits for stabilization

For the stabilization of the dither, two types of compensating circuits can be considered in the feedback circuit. One is a low-pass filter which cuts off the feedback of the dither components. The other is a phase lead network which compensates the pulse transmission lag in the forward circuit of the servomechanism. The stability problems for the case when compensating circuits are used in a feedback circuit are discussed as follows.

5.1. Compensation by a first-order system

A first-order system is a simple and representative circuit in low-pass filters. The transfer function is given by

$$G_f(j\omega) = \frac{K_f}{1 + T_f j\omega}. \tag{45}$$

In this case, stabilities of both the servo loop and the dither must be considered.

(1) Stability of the servo loop

Using Eqs. (39) and (45), the following equation is obtained:

$$\omega_l t_{D_0} + \tan^{-1}(T_f \omega_l) = \pi/2. \tag{46}$$

If ω_l calculated by Eq. (46) satisfys the relation of $\omega_l T_0 < \pi$, the stability of the servo loop must be considered. In this case, the gain at the stability limit is obtained by Eq. (40). Substituting $K_v = v_m/y_m$ and Eqs. (37), (45) and (46) into Eq. (40) leads to

$$K_f k v_m \cos\left(\frac{\omega_l T_0}{4}\right) \sin(\omega_l t_{D_0}) = \omega_l. \tag{47}$$

Therefore, the critical loop gain is given by

$$T_0 v_m K_f k = \frac{\omega_l T_0}{\cos(\omega_l T_0/4) \sin(\omega_l t_{D_0})}. \tag{48}$$

(2) Stability of the dither

Substituting the gain and the phase angle obtained by Eq. (45) into Eqs. (43) and (44), the critical loop gains are obtained as follows:

When $\left\{ t_{D_0} + \dfrac{T_0}{2\pi} \tan^{-1}\left(\dfrac{2\pi T_f}{T_0}\right) \right\} < \dfrac{T_0}{4}$,

$$T_0 v_m K_f k = \frac{\sqrt{1 + 4\pi^2 (T_f/T_0)^2}}{\dfrac{t_{D_0}}{T_0} + \dfrac{1}{2\pi} \tan^{-1}\left(\dfrac{2\pi T_f}{T_0}\right)}. \tag{49}$$

When $\quad \dfrac{T_0}{4} < \left\{t_{D0} + \dfrac{T_0}{2\pi}\tan^{-1}\left(\dfrac{2\pi T_f}{T_0}\right)\right\} < \dfrac{3}{4}\,T_0$,

$$T_0 v_m K_f k = 2\sqrt{1 + 4\pi^2(T_f/T_0)^2}\,. \tag{50}$$

(3) Design of a compensating circuit of a first-order system

In Fig. 14, the solid curves show the stability limits of the dither calculated by Eqs. (49) and (50), the broken curves being those of the servo loop calculated by Eq. (48). Both groups of these curves are distinguished by T_f/T_0. If both the pulse period and time constant of the first-order system are constant, the loop gain must be adjusted to be in the left range of both the solid and broken curves which have the same parameters. The chain curve in Fig. 14 is the locus of the intersections of the solid and broken curves for the same T_f/T_0, and it gives the maximum loop gain for various t_{D0}/T_0. Fig. 15 shows the optimum time constants which give the maximum gains represented by the chain curve in Fig. 14.
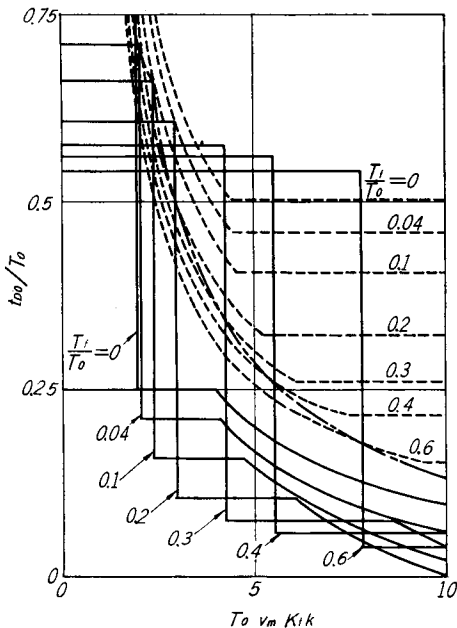

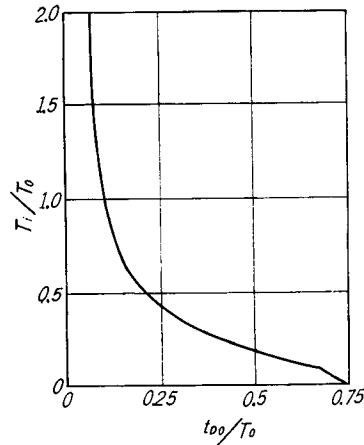Fig. 14. Effects of compensations by a first-order system.

Fig. 15. Optimum time constants of a first-order system.

5.2. Compensation by a phase lead network

A phase lead network compensates the pulse transmission lag in the forward circuit of the servomechanism, and reduces the phase lag of the overall system. The transfer function of the phase lead network is represented by

$$G_f(s) = \frac{K_f(1 + T_{f1}s)}{1 + T_{f2}s} \tag{51}$$

where $T_{f1} > T_{f2}$. When the feedback circuit consists of a phase lead network, the servo loop becomes more stable than in the case when the feedback circuit

consists of a proportional element. Therefore, the stability limit is determined by the stability of the dither. Two typical types of phase lead networks are considered to stabilize the dither.

(1) Phase lead network which has the maximum phase lead for the dither component

When the phase lead network is designed to have the maximum phase lead for the dither component of the period T_0, the transfer function of Eq. (51) is reduced to

$$G_f(s) = \frac{K_f(1 + T_{f_1}s)}{1 + \left(\frac{T_0}{2\pi}\right)^2 \frac{s}{T_{f_1}}}. \quad (52)$$

Substituting the gain and the phase angle obtained by Eq. (52) into Eqs. (43) and (44), the critical loop gains are obtained as follows:

When

$$t_{D0} - \frac{T_0}{2\pi}\left\{\tan^{-1}\left(\frac{2\pi T_{f_1}}{T_0}\right) - \tan^{-1}\left(\frac{T_0}{2\pi T_{f_1}}\right)\right\} < \frac{T_0}{4},$$

$$T_0 v_m K_f k = \frac{1}{2\pi} \frac{T_0}{T_{f_1}}\left[\frac{t_{D0}}{T_0} - \frac{1}{2\pi}\left\{\tan^{-1}\left(\frac{2\pi T_{f_1}}{T_0}\right)\right.\right.$$
$$\left.\left. - \tan^{-1}\left(\frac{T_0}{2\pi T_{f_1}}\right)\right\}\right]^{-1}. \quad (53)$$

When

$$\frac{3}{4}T_0 > t_{D0} - \frac{T_0}{2\pi}\left\{\tan^{-1}\left(\frac{2\pi T_{f_1}}{T_0}\right)\right.$$
$$\left. - \tan^{-1}\left(\frac{T_0}{2\pi T_{f_1}}\right)\right\} > \frac{T_0}{4},$$

$$T_0 v_m K_f k = T_0/\pi T_{f_1}. \quad (54)$$

In Fig. 16, the solid curves show the stability limits of the dither calculated by Eqs. (53) and (54) for various values of T_{f_1}/T_0. The broken curves show the limit of the compensation by the phase lead network which has the maximum phase lead for the dither component. Fig. 17 shows the optimum time constant which gives the maximum gain represented by the broken curve in Fig. 16.
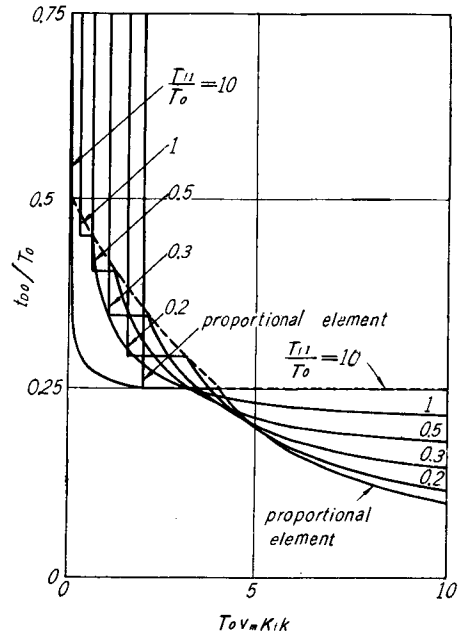

Fig. 16. Effects of compensations by a phase lead network with a maximum phase lead for a dither component.
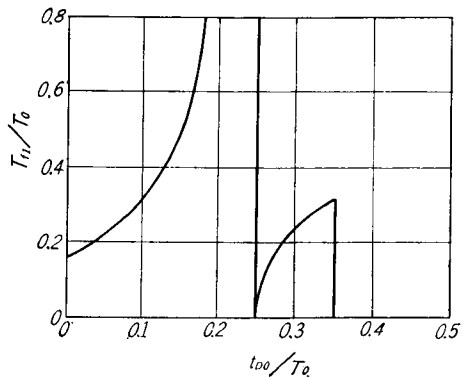

Fig. 17. Optimum time constants of a phase lead network with a maximum phase lead for a dither component.

(2)　Phase lead network in which the ratio of T_{f2} to T_{f1} is constant

In this case, the transfer function is represented as

$$G_f(s) = \frac{K_f(1+T_{f1}s)}{1+nT_{f1}s} \tag{55}$$

where $n=$constant and $n<1$. Substituting the gain and the phase angle obtained by Eq. (55) into Eqs. (43) and (44), the critical loop gains are obtained as follows:

When　　$t_{D0} - \dfrac{T_0}{2\pi}\left\{\tan^{-1}\left(\dfrac{2\pi T_{f1}}{T_0}\right) - \tan^{-1}\left(\dfrac{2\pi n T_{f1}}{T_0}\right)\right\} < \dfrac{T_0}{4}$,

$$T_0 v_m K_f k = \left[\frac{t_{D0}}{T_0} - \frac{1}{2\pi}\left\{\tan^{-1}\left(\frac{2\pi T_{f1}}{T_0}\right) - \tan^{-1}\left(\frac{2n\pi T_{f1}}{T_0}\right)\right\}\right]^{-1}$$
$$\times \sqrt{\frac{1+(2n\pi T_{f1}/T_0)^2}{1+(2\pi T_{f1}/T_0)^2}}. \tag{56}$$

When　　$\dfrac{3}{4}T_0 > t_{D0} - \dfrac{T_0}{2\pi}\left\{\tan^{-1}\left(\dfrac{2\pi T_{f1}}{T_0}\right) - \tan^{-1}\left(\dfrac{2n\pi T_{f1}}{T_0}\right)\right\} > \dfrac{T_0}{4}$,

$$T_0 v_m K_f k = 2\sqrt{\frac{1+(2n\pi T_{f1}/T_0)^2}{1+(2\pi T_{f1}/T_0)^2}}. \tag{57}$$

Fig. 18 shows the stability limits of the dither calculated by Eqs. (56) and (57) for various values of T_{f1}/T_0 and $n=0.5$. In this case, the optimum time constants are obtained by substituting Eq. (56) into $d(T_0 v_m K_f k)/d(T_{f1}/T_0) = 0$. Then, the relation between t_{D0}/T_0 and the optimum value of T_{f1}/T_0 is obtained as
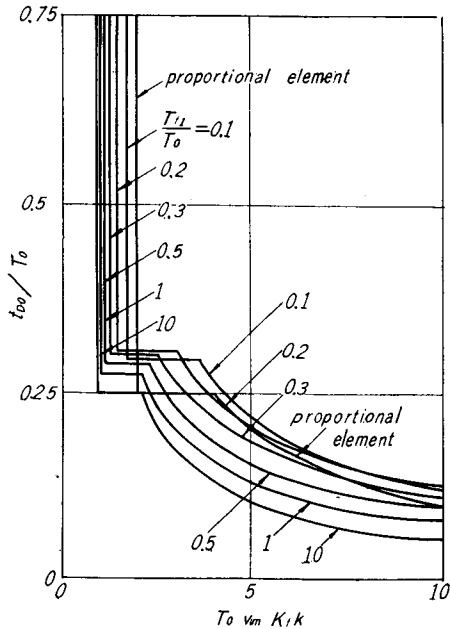
$$\frac{t_{D0}}{T_0} = \frac{1}{2\pi}\left\{\tan^{-1}\left(\frac{2\pi T_{f1}}{T_0}\right)\right.$$
$$\left. - \tan^{-1}\left(\frac{2n\pi T_{f1}}{T_0}\right)\right\} + \frac{1-4\pi^2 n(T_{f1}/T_0)^2}{4\pi^2(n+1)(T_{f1}/T_0)^2} \tag{58}$$

Fig. 19 shows the relations of t_{D0}/T_0 and T_{f1}/T_0 obtained by Eq. (58).

Fig. 18.　Effects of compensations by a phase lead network in which the ratio of T_{f_2} to T_{f_1} is constant.
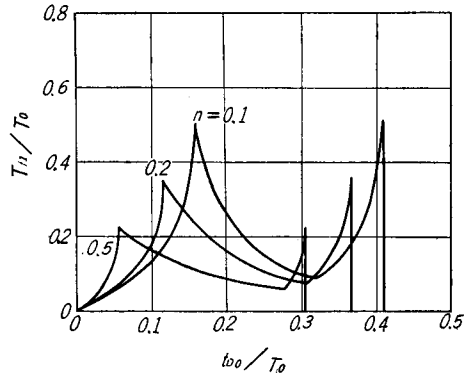

Fig. 19.　Optimum time constants of a phase lead network in which the ratio of T_{f_2} to T_{f_1} is constant.

5.3. Comparison of the compensating circuits

By the preceding analysis, the stability limits are obtained for three types of compensating circuits, and the optimum time constants are determined for every compensating circuit. In Fig. 20, Curve (1) shows the stability limit for the feedback circuit of the proportional element, Curve (2) showing that for the first-order system, Curve (3) showing that for the phase lead network with the maximum phase lead, and Curve (4) indicates that for the phase lead network of $n=$constant. By comparison of these curves, it is seen that phase lead networks are suitable for the case when t_{D0}/T_0 is small. The first order system is effective in each case, and is particularly suitable for the case when t_{D0}/T_0 is larger than 1/4.
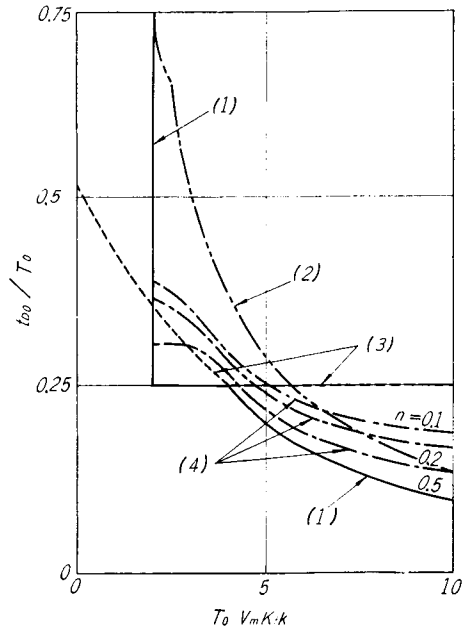

Fig. 20. Comparison of compensations by various circuits.

6. Compensation of the servomechanism in which the controlled system consists of a first-order one

The block diagram of the servomechanism is shown in Fig. 21. Though the lag characteristics contained in the controlled system are effective to reduce the amplitude of the dither in the output, it causes instability of the servo loop and the dither. In this case,

Fig. 21. Block diagram of a servomechanism with a first-order controlled system.

the compensating circuit of Eq. (51) is used, and the time constants are determined by referring to the preceding analysis.
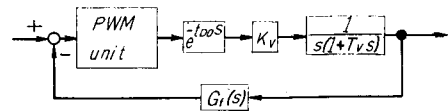
6.1. When $t_{D0}+\dfrac{T_0}{2\pi}\tan^{-1}\left(\dfrac{2\pi T_v}{T_0}\right)<\dfrac{T_0}{4}$

This case corresponds to the case of $t_{D0}/T_0<1/4$ in the preceding analysis. In this case, the most effective compensation is that by the phase lead network which has the maximum phase lead for the dither component of the period T_0. When this network is used, the stability limit is given by

$$T_0 v_m K_f k = \frac{T_0}{2\pi T_{f1}} \sqrt{1 + \left(\frac{2\pi T_v}{T_0}\right)^2} \left[\frac{t_{D0}}{T_0} + \frac{1}{2\pi} \left\{ \tan^{-1}\left(\frac{2\pi T_v}{T_0}\right) \right.\right.$$
$$\left.\left. - \tan^{-1}\left(\frac{2\pi T_{f1}}{T_0}\right) + \tan^{-1}\left(\frac{T_0}{2\pi T_{f1}}\right) \right\} \right]^{-1}. \qquad (59)$$

In this case, both the phase lead network of n = constant and the first-order system are also effective. The time constants of these compensating circuits are determined by Fig. 15, Fig. 17 and Fig. 19, if the abscissas are replaced by $\left\{ \frac{t_{D0}}{T_0} + \frac{1}{2\pi} \tan^{-1}\left(\frac{2\pi T_v}{T_0}\right) \right\}$.

6. 2.   When $\dfrac{3}{4} T_0 > t_{D0} + \dfrac{T_0}{2\pi} \tan^{-1}\left(\dfrac{2\pi T_v}{T_0}\right) > \dfrac{T_0}{4}$

This case corresponds to the case of $3/4 > t_{D0}/T_0 > 1/4$ in the preceding analysis. In this case, the most effective compensation is to replace the time constant T_v in the controlled system by the optimum time constant T_f given by Fig. 15. The transfer function of the feedback circuit is given by the following:

$$G_f(s) = \frac{K_f(1 + T_v s)}{1 + T_f s}. \qquad (60)$$

7.   Experiments

Experiments were carried out by an electrohydraulic servomechanism as shown in Fig. 22. Principal dimensions are as follows:

Displacement of a spool = ±0.3 mm
Width of a control orifice in a spool
      valve = 2 mm
Area of an actuator piston = 10 cm²
Friction of an actuator piston = 9 kg
Supply pressure = 30 kg·cm⁻²
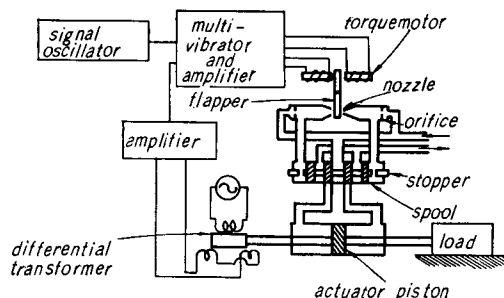$t_{D0} = 4.5$ ms $k = 0.22$ v⁻¹ $v_m = 2.2$ cm·s⁻¹ .

Fig. 22.   Schematic diagram of an electrohydraulic servomechanism operated by a PWM mode.

7. 1.   Waveshape-change of a dither in a fundamental circuit

Waveshapes of the dither of the actuator piston are shown in Fig. 23 for two pulse periods and for various gain constants of the feedback loop. When $T_0 =$ 18.3 ms, t_{D0} becomes smaller than $T_0/4$, and it is expected theoretically that the triangular wave of the period T_0 continues so far as $K_f = 45.8$ v·mm⁻¹, and that the triangular wave of the period $2T_0$ takes place for $K_f \geq 45.8$ v·mm⁻¹. When $T_0 = 11.4$ ms, t_{D0} becomes larger than $T_0/4$, and it is expected that the triangular
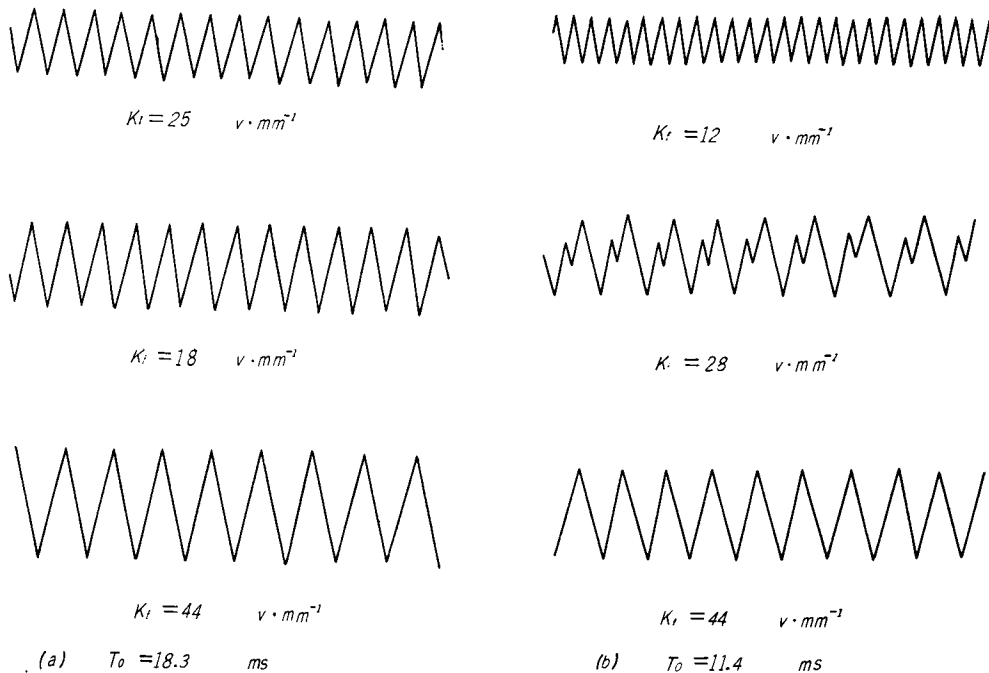
$K_f = 25 \quad v \cdot mm^{-1}$

$K_f = 12 \quad v \cdot mm^{-1}$

$K_f = 18 \quad v \cdot mm^{-1}$

$K_f = 28 \quad v \cdot mm^{-1}$

$K_f = 44 \quad v \cdot mm^{-1}$

$K_f = 44 \quad v \cdot mm^{-1}$

(a) $T_0 = 18.3$ ms

(b) $T_0 = 11.4$ ms

Fig. 23. Waveshape-change of dithers for a fundamental circuit.

wave of the period T_0 continues so far as $K_f = 36.2$ v·mm^{-1}, that the disturbed wave occurs for $K_f = 36.2 \sim 45.8$ v·mm^{-1}, and that the triangular wave occurs over $K_f = 45.8$ v·mm^{-1}. Fig. 23 shows such changes of the waveshapes as expected.

Fig. 24 shows the maximum displacements of the actuator piston for $T_0 = 18.3$ ms and $T_0 = 11.4$ ms. When $T_0 = 18.3$ ms, the displacement for small values of K_f is not constant, but it increases gradually with K_f. This is different from the theoretical analysis because the multivibrator in Fig. 22 modulates not strictly but approximately the pulse width depending on the principle of the symmetrical modulation. However, it was verified by experiments that the dither in the displacement of the actuator
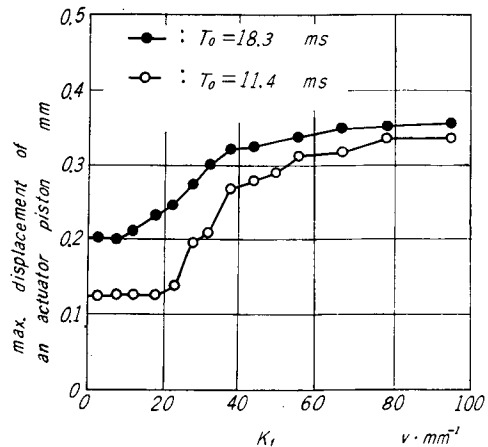

Fig. 24. Maximum displacements of an actuator piston in a fundamental circuit.

piston became unstable for certain loop gains, and that the various waveshapes of the dither took place as was expected theoretically.

7. 2. Compensation by a first-order system

The circuit of a first-order system is shown in Fig. 25. In Table 2, the optimum values of C_f in the circuit are shown for $T_0 = 18.3$ ms, 16.8 ms and 11.4 ms, which were determined by the theoretical calculations and the experiments. The maximum displacements of the actuator piston are

Fig. 25. Compensating circuit of a first-order system.

shown in Fig. 26 and Fig. 27 for $T_0 = 18.3$ ms and $T_0 = 11.4$ ms, respectively. In these figures, the curves for $C_f = 0$ represent the case when the feedback circuit consists of a proportional element. As the pulse transmission lag t_{D0} is 4.5 ms in this apparatus, t_{D0}/T_0 is smaller than $1/4$ for $T_0 = 18.3$ ms, and exists between $1/4$ and $1/2$ for $T_0 = 11.4$ ms. In both cases, it is seen that the first-order systems are effective to stabilize the servo mechanism.
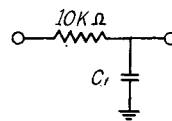
Table 2. Optimum values of C_f in first-order systems.

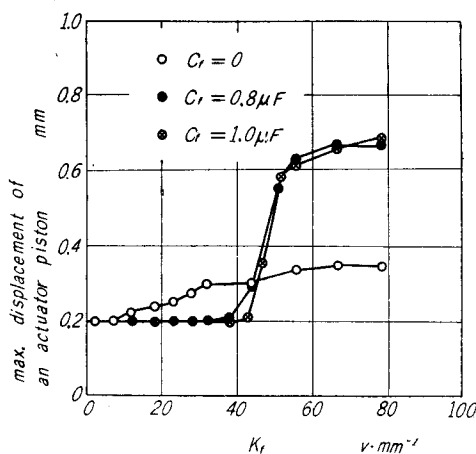| T_0 (ms)	$\dfrac{t_{D0}}{T_0}$	C_f (μF)	
		Theoretical	Experimental
18.3	0.244	0.77	0.8 ~ 1.0
16.8	0.268	0.66	0.6 ~ 0.8
11.4	0.394	0.29	0.2 ~ 0.4

Fig. 26. Maximum displacement of an actuator piston in a compensated circuit by a first-order system for $T_0 = 18.3$ ms.
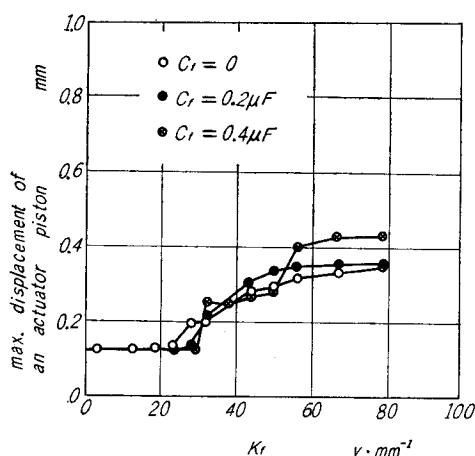
Fig. 27. Maximum displacements of an actuator piston in a compensated circuit by a first-order system for $T_0 = 11.4$ ms.

7.3. Compensation by a phase lead network

The circuit of a phase lead network is shown in Fig. 28. The transfer function of this network is represented by Eq. (55). In Table 3, the optimum values of C_f are shown for $T_0 = 25.4$ ms and 17.0 ms. When the phase lead networks of the optimum time constants are used for the compensation, the waveshapes of the dithers are always triangular.
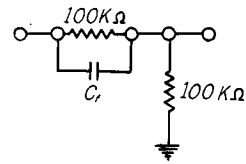

Fig. 28. Compensating circuit of a phase lead network.

Table 3. Optimum values of C_f in phase lead networks.

T_0 (ms)	$\dfrac{t_{D_0}}{T_0}$	C_f (μF) Theoretical	C_f (μF) Experimental
25.4	0.177	0.03	0.08
17.0	0.265	0.01	0.03
13.9	0.374	—	—

Table 4. Change of a dither period for $T_0 = 25.4$ ms.

K_f (v·mm^{-1})	Dither period (ms) $C_f = 0$	Dither period (ms) $C_f = 0.08\ \mu$F
2.5	25.4	25.4
12	30.2	28.4
23	33.3	28.6
32	35.1	29.0
44	35.7	29.0
56	36.3	29.2
67	36.3	29.6
79	36.3	30.2
95	36.3	30.2

Table 5. Change of a dither period for $T_0 = 17.0$ ms.

K_f (v·mm^{-1})	Dither period (ms) $C_f = 0$	Dither period (ms) $C_f = 0.03\ \mu$F
2.5	17.0	17.0
12	18.9	18.7
23	22.2	23.0
32	27.2	24.8
44	28.4	25.4
56	30.2	25.4
67	31.5	25.4
79	31.5	25.4
95	31.5	25.4

Table 6. Change of a dither period for $T_0 = 13.9$ ms.

K_f (v·mm^{-1})	Dither period (ms) $C_f = 0$	Dither period (ms) $C_f = 0.03\ \mu$F
2.5	13.9	13.9
12	15.0	16.3
23	16.7	21.0
32	21.7	24.3
44	25.4	25.1
56	27.8	25.8
67	29.0	25.8
79	29.0	25.8
95	29.0	25.8

Therefore, the maximum displacements of the actuator piston are proportional to the dither periods. The periods of the dithers are shown in Table 4, Table 5 and Table 6 for $T_0 = 25.4$ ms, 17.0 ms and 13.9 ms, respectively. In these tables, the columns of $C_f = 0$ represent the case when the feedback circuit consists of a proportional element. When $T_0 = 25.4$ ms and 17.0 ms, the phase lead networks are effective to stabilize the dither. However, when $T_0 = 13.9$ ms, the dither tends to be unstable by the phase lead network. These are expected by the theoretical analysis.

8. Conclusion

The output displacement of the servomechanism operated by the PWM mode contains the dither corresponding to the carrier pulse. When the loop gain becomes high, the dither component which is fed back through the feedback circuit has an effect on the pulse modulation and the waveshape of the dither in the output is disturbed. In this paper, the stabilities of both the dither and the servo loop were studied.

In the fundamental circuit in which the feedback circuit consists of a proportional element, we may consider only the stability of the dither in the output. In this case, it was shown that the various waveshapes took place depending on the ratio of the pulse transmission lag to the pulse period and the loop gain. The ranges of the loop gain were also obtained for the various waves.

Next, the stabilities of the dither and the servo loop were studied for the case when the compensating circuits were used in the feedback circuit. Two types of the compensating circuits were considered: one was a first-order system and the other was a phase lead network. It was shown that these circuits were effective for stabilizing the servomechanism, if they were selected properly according to the ratio of the pulse transmission lag and the carrier pulse period. The optimum time constants were given for every compensating circuit. Finally, the theoretical results were verified by experiments which were carried out by an electrohydraulic servomechanism.

Acknowledgement

References

1) J. E. Gibson and F. B. Tuteur : "Control System Components", McGRAW-HILL, New York, p. 389 (1958).
2) S. A. Murtaugh : Trans. ASME, J. of Basic Engg., **Vol. 81,** Series D, No. 2, p. 263 (1959).
3) T. Sawamura, H. Hanafusa and T. Inui : THESE MEMOIRS, **22,** 123 (1960).
4) T. Sawamura, H. Hanafusa and T. Inui : THESE MEMOIRS, **22,** 1 (1960).